NASA Technical Memorandum 4026

Delamination Stresses in Semicircular Laminated Composite Bars

William L. Ko

JANUARY 1988

NASA

NASA Technical Memorandum 4026

Delamination Stresses in Semicircular Laminated Composite Bars

William L. Ko
Ames Research Center
Dryden Flight Research Facility
Edwards, California

National Aeronautics
and Space Administration

Scientific and Technical
Information Division

1988

CONTENTS

SUMMARY 1

INTRODUCTION 1

NOMENCLATURE 1

COMPOSITE CURVED BAR 2

ANISOTROPIC CURVED BAR UNDER END FORCES 2
Stresses Induced 3
Location of Maximum σ_r 4
Thin Curved Bar 5

ANISOTROPIC CURVED BAR UNDER END MOMENTS 5
Stresses Induced 6
Location of Maximum σ_r' 7
Thin Curved Bar 8

DELAMINATION STRESS 8

NUMERICAL RESULTS 9

CONCLUDING REMARKS 12

APPENDIX—EXPANSION OF STRESS EQUATIONS (26) AND (27) FOR ISOTROPIC CASE ($k = 1$) 13
Expansion of C 13
Expansion of σ_r' 14

REFERENCES 15

SUMMARY

Using anisotropic elasticity theory, delamination stresses in a semicircular laminated composite curved bar subjected to end forces and end moments were calculated, and their radial locations were determined. A family of design curves was presented, showing variation of the intensity of delamination stresses and their radial locations with different geometry and different degrees of anisotropy of the curved bar. The effect of anisotropy on the location of peak delamination stress was found to be small.

INTRODUCTION

The major cause of degradation in stiffness and strength of laminated composite materials is the growth of delamination between individual composite layers. Excess delamination may result in ultimate fatigue failure. The most common failure mode of laminated composite material is delamination failure. Delamination may result from the following: eccentricities in the structural load paths, inducing out-of-plane loads; discontinuities in the structure, creating local out-of-plane loads; low-velocity impacts; cyclic loading; incomplete curing; and the introduction of foreign particles during the manufacturing process. The delamination growth may redistribute stresses in the composite plies and therefore may reduce the residual stiffness and strength of the laminated composites. In the common application of the composite materials, many structural parts have certain degrees of curvature. Because of this curvature, radial stress can be generated. If the radial stress is in tension, this stress will function as open-mode delamination stress and will cause the delamination to initiate and grow under service loading (mostly cyclic loading).

Delamination problems in composite materials have been studied extensively recently, and major research activities are listed in O'Brien (1984a). There are a variety of ways to conduct composite delamination studies using different types of test specimens. However, one of the most attractive test coupon geometries is in the shape of a semicircular curved bar. It is well known that if the curved bar is subjected to bending, radial stress and shear stress can be induced inside the curved bar. If the loading is intense enough, open-mode delamination can take place at the site of peak tensile radial stress. If the composite curved bar has weak shear strength, shear-mode delamination can occur at the site of peak shear stress. Since the peak value of tensile radial stress (or peak shear stress) occurs only at a particular point, the curved bar offers an excellent situation for studying the initiation and subsequent growth of delamination under cyclic loading and the fatigue behavior (degradation of stiffness and strength) of laminated composite materials.

The purpose of this report is to document the calculation of delamination stress (open-mode or shear mode) and its exact radial location and to relate how delamination stress and its location change with the degree of anisotropy (different stacking sequences) and the wall thickness of the curved bar.

NOMENCLATURE

a	inner radius of curved bar, in
b	outer radius of curved bar, in
E_{L}	modulus of elasticity of single ply in fiber direction, lb/in^2
E_r	modulus of elasticity of laminated composite in r direction, lb/in^2
E_{T}	modulus of elasticity of single ply in direction transverse to fiber direction, lb/in^2
E_θ	modulus of elasticity of laminated composite in θ direction, lb/in^2
e	loading axis offset, in
G_{LT}	shear modulus of single ply, lb/in^2
$G_{\theta r}$	shear modulus of laminated composite, lb/in^2
h	width of curved bar, in

k	anisotropic parameter, $\sqrt{E_\theta/E_r}$
M	applied end moment, in-lb
P	applied end force, lb
r	radial coordinate, in
r_m	radial location of $(\sigma_r)_{max}$, in
r'_m	radial location of $(\sigma'_r)_{max}$, in
t	thickness of curved bar, $t = (b - a)$, in
β	anisotropic parameter, $\beta = \sqrt{1 + (E_\theta/E_r)(1 + 2\nu_{\theta r}) + E_\theta/G_{\theta r}}$
θ	tangential coordinate, rad
ν_{LT}, ν_{TL}	Poisson ratios of single-layer composite
$\nu_{\theta r}$	Poisson ratio of laminated composite
σ_D	maximum radial stress (open-mode delamination stress) induced by both P and M, $\sigma_D = (\sigma_r)_{max} + (\sigma'_r)_{max}$, lb/in^2
σ_r	radial stress induced by end forces P, lb/in^2
σ'_r	radial stress induced by end moments M, lb/in^2
$(\sigma_r)_{max}$	maximum radial stress induced by end forces P, lb/in^2
$(\sigma'_r)_{max}$	maximum radial stress induced by end moments M, lb/in^2
σ_θ	tangential stress induced by end forces P, lb/in^2
σ'_θ	tangential stress induced by end moments M, lb/in^2
$\tau_{r\theta}$	shear stress induced by end forces P, lb/in^2
$\tau'_{r\theta}$	shear stress induced by end moments M, lb/in^2

COMPOSITE CURVED BAR

Figure 1 shows a semicircular composite curved bar subjected to end forces P. Because finite area is needed for load attachment in the fatigue tests, both ends of the curved bar have to be extended slightly. Thus, the loading axis will have slight offset e from the vertical diameter of the curved bar. Therefore, the loading state in figure 1 (or fig. 2, A) is the combination of two cases:

1. Bending due to end forces P with the loading axis coinciding with the vertical diameter of the curved bar (fig. 2, B)
2. Pure bending due to end moments $M\,(= Pe)$ created by the loading axis offset e (fig. 2, C)

It has been observed that the highest probability of delamination onset takes place at the interfaces of 0° and 90° plies because of high Poisson's ratio mismatch (O'Brien, 1982; O'Brien, 1984b). In constructing the curved-bar test coupon, it is desirable to introduce 90° plies at, or in the vicinity of, a peak stress point (that is, a peak radial tensile stress point or peak shear stress point) and thereby ensure that the delamination will initiate at the peak stress point, which is yet to be determined. In the following sections, the peak radial tensile stress (or peak shear stress) and its radial location will be calculated.

ANISOTROPIC CURVED BAR UNDER END FORCES

Figure 3 shows the anisotropic semicircular curved bar subjected to end forces P with the loading axis coinciding with the vertical diameter of the curved bar. The situation in figure 3 is similar to that in figure 2, B.

Stresses Induced

If the composite material of the curved bar is treated as a continuous anisotropic material, then the stresses induced in the composite curved bar due to the end forces P may be written as (Lekhnitshii and others, 1968, p. 99, taking $\omega = 0°$)

$$\sigma_r(r,\theta) = \frac{P}{bhg_1}\frac{b}{r}\left[\left(\frac{r}{b}\right)^{\beta} + \left(\frac{a}{b}\right)^{\beta}\left(\frac{b}{r}\right)^{\beta} - 1 - \left(\frac{a}{b}\right)^{\beta}\right]\sin\theta \tag{1}$$

$$\sigma_\theta(r_1\theta) = \frac{P}{bhg_1}\frac{b}{r}\left[(1+\beta)\left(\frac{r}{b}\right)^{\beta} + (1-\beta)\left(\frac{b}{r}\right)^{\beta}\left(\frac{a}{b}\right)^{\beta} - 1 - \left(\frac{a}{b}\right)^{\beta}\right]\sin\theta \tag{2}$$

$$\tau_{r\theta}(r_1\theta) = \frac{P}{bhg_1}\frac{b}{r}\left[\left(\frac{r}{b}\right)^{\beta} + \left(\frac{a}{b}\right)^{\beta}\left(\frac{b}{r}\right)^{\beta} - 1 - \left(\frac{a}{b}\right)^{\beta}\right]\cos\theta \tag{3}$$

where

- a is inner radius of the curved bar,
- b outer radius of the curved bar,
- h width of the curved bar,
- r radial coordinate,
- θ tangential coordinate,
- σ_r radial stress,
- σ_θ tangential stress,
- $\tau_{r\theta}$ shear stress,

and

$$g_1 = \frac{2}{\beta}\left[1 - \left(\frac{a}{b}\right)^{\beta}\right] + \left[1 + \left(\frac{a}{b}\right)^{\beta}\right]\ln\frac{a}{b} \tag{4}$$

and the anisotropic parameter β is defined as

$$\beta = \sqrt{1 + \frac{E_\theta}{E_r}(1 - 2\nu_{\theta r}) + \frac{E_\theta}{G_{\theta r}}} \tag{5}$$

where

- E_θ is modulus of elasticity in θ direction,
- E_r modulus of elasticity in r direction,
- $G_{\theta r}$ shear modulus, and
- $\nu_{\theta r}$ Poisson's ratio.

For isotropic materials, $\beta = 2$.

Notice from equations (1) and (3) that the magnitudes of σ_r and $\tau_{r\theta}$ are identical, but they are out of phase by $\pi/2$. The maximum value of σ_r occurs at cross section $\theta = \pi/2$ (midspan of the curved bar), and $\tau_{r\theta}$ reaches its peak value at the two load application cross sections $\theta = 0$ and $\theta = \pi$:

$$\sigma_r\left(r, \frac{\pi}{2}\right) = -\tau_{r\theta}(r,0) = \tau_{r\theta}(r,\pi) \tag{6}$$

Thus, the semicircular curved-bar test coupon can provide the same intensities of open-mode and shear-mode delamination stresses simultaneously. If the composite is weak in open-mode strength, the delamination will initiate at the midspan $\theta = \pi/2$. On the other hand, if the composite is weak in shear strength, delamination will start at both ends of the curved bar (that is, $\theta = 0$ and $\theta = \pi$).

Because of the relationship between σ_r and $\tau_{r\theta}$ given in equation (6), analysis will be limited to σ_r. Equation (1) (for $\theta = \pi/2$) may be rewritten as

$$\sigma_r\left(r, \frac{\pi}{2}\right) = \frac{P}{haB}\frac{a}{r}\left[\left(\frac{r}{a}\right)^{\beta} + \left(\frac{b}{a}\right)^{\beta}\left(\frac{a}{r}\right)^{\beta} - \left(\frac{b}{a}\right)^{\beta} - 1\right] \tag{7}$$

where

$$B \equiv \frac{2}{\beta}\left[\left(\frac{b}{a}\right)^{\beta} - 1\right] - \left[\left(\frac{b}{a}\right)^{\beta} + 1\right]\ln\frac{b}{a} \tag{8}$$

Or, in dimensionless form,

$$\frac{h(b-a)}{P}\sigma_r\left(r, \frac{\pi}{2}\right) = \frac{(b/a-1)}{B}\frac{a}{r}\left[\left(\frac{r}{a}\right)^{\beta} + \left(\frac{b}{a}\right)^{\beta}\left(\frac{a}{r}\right)^{\beta} - \left(\frac{b}{a}\right)^{\beta} - 1\right] \tag{9}$$

For the isotropic case (that is, $\beta = 2$), equation (7) may be written in the following form (for $h = 1$):

$$\left[\sigma_r\left(r, \frac{\pi}{2}\right)\right]_{\beta=2} = -\frac{P}{N}\left[r + \frac{a^2b^2}{r^3} - \frac{1}{r}(a^2 + b^2)\right] \tag{10}$$

where

$$N = -a^2(B)_{\beta=2} = a^2 - b^2 + (a^2 + b^2)\ln\frac{b}{a} \tag{11}$$

Notice that equation (10) is identical with the expression given by Timoshenko and Goodier (1970) for isotropic materials).

Location of Maximum σ_r

The radial location $r = r_m$ where $\sigma_r(r, \pi/2)$ reaches its peak value $(\sigma_r)_{max}$ may be found by differentiating equation (7) with respect to r and setting the resulting derivative to zero, or

$$\frac{d}{dr}\left[\sigma_r\left(r, \frac{\pi}{2}\right)\right] = 0 \tag{12}$$

from which r_m is found as

$$\left(\frac{r_m}{a}\right)^{\beta} = \frac{1}{2(\beta-1)}\left\{\sqrt{\left[\left(\frac{b}{a}\right)^{\beta} + 1\right]^2 + 4(\beta^2 - 1)\left(\frac{b}{a}\right)^{\beta}} - \left[\left(\frac{b}{a}\right)^{\beta} + 1\right]\right\} \tag{13}$$

For the isotropic case

$$\left(\frac{r_m}{a}\right)^2 = \frac{1}{2}\left\{\sqrt{\left[\left(\frac{b}{a}\right)^2 + 1\right]^2 + 12\left(\frac{b}{a}\right)^2} - \left[\left(\frac{b}{a}\right)^2 + 1\right]\right\} \tag{14}$$

$(\sigma_r)_{\max}$ may be written as

$$\frac{h(b-a)}{P}(\sigma_r)_{\max} = \frac{h(b-a)}{P}\,\sigma_r\left(r_m, \frac{\pi}{2}\right) = \frac{(b/a-1)}{B}\frac{a}{r_m}\left[\left(\frac{r_m}{a}\right)^{\beta} + \left(\frac{b}{a}\right)^{\beta}\left(\frac{a}{r_m}\right)^{\beta} - \left(\frac{b}{a}\right) - 1\right] \tag{15}$$

where r_m is given by equation (13).

Thin Curved Bar

When the thickness $t\ (= b - a)$ of the curved bar is small,

$$\frac{b}{a} = 1 + \frac{t}{a} \qquad \left(\frac{t}{a}\right) \ll 1 \tag{16}$$

The expression for B given in equation (8) may be expanded in terms of small quantity t/a as

$$(B)_{b\to a} = -\frac{1}{6}\left(\frac{t}{a}\right)^3 \beta^2 + \cdots \tag{17}$$

Notice that the lower order terms up to $O(t/a)^2$ cancelled out.

The expression for r_m given in equation (13) may be expanded to the following form:

$$\left(\frac{r_m}{a}\right)_{b\to a} = 1 + \frac{1}{2}\frac{t}{a} - \frac{1}{4}\left(\frac{t}{a}\right)^2 + \cdots \tag{18}$$

Notice that r_m is independent of β and that $(\sigma_r)_{\max}$ is always located on the inner side of the middle surface of the curved bar.

Lastly, equation (15), with equation (18) applied, may be expanded as

$$\left[\frac{h(b-a)}{P}(\sigma_r)_{\max}\right]_{b\to a} = -\frac{1}{B}\left(\frac{t}{a}\right)^3 \frac{\beta^2}{4} + \cdots \tag{19}$$

where the lower order terms up to $O(t/a)^2$ cancelled out.

Combining equations (17) and (19) there results

$$\left[\frac{h(b-a)}{P}(\sigma_r)_{\max}\right]_{b\to a} = \frac{3}{2} \tag{20}$$

which is independent of anisotropy (that is, the value of β).

ANISOTROPIC CURVED BAR UNDER END MOMENTS

Figure 4 shows the anisotropic semicircular curved bar under pure bending due to end moments M. This case corresponds to that in figure 2, C.

Stresses Induced

If the composite material of the curved bar is treated as continuous anisotropic material, the radial stress σ'_r, tangential stress σ'_θ, and shear stress $\tau'_{r\theta}$ induced in the curved bar under the end moments M may be expressed as (Lekhnitskii and others, 1968, p. 97)

$$\sigma'_r(r) = -\frac{M}{b^2hg}\left[1 - \frac{1-(a/b)^{k+1}}{1-(a/b)^{2k}}\left(\frac{r}{b}\right)^{k-1} - \frac{1-(a/b)^{k-1}}{1-(a/b)^{2k}}\left(\frac{a}{b}\right)^{k+1}\left(\frac{b}{r}\right)^{k+1}\right] \tag{21}$$

$$\sigma'_\theta(r) = -\frac{M}{b^2hg}\left[1 - \frac{1-(a/b)^{k+1}}{1-(a/b)^{2k}}k\left(\frac{r}{b}\right)^{k-1} + \frac{1-(a/b)^{k-1}}{1-(a/b)^{2k}}k\left(\frac{a}{b}\right)^{k-1}\left(\frac{b}{r}\right)^{k+1}\right] \tag{22}$$

$$\tau'_{r\theta} = 0 \tag{23}$$

where the anisotropic parameter k is defined by

$$k = \sqrt{\frac{E_\theta}{E_r}} \tag{24}$$

and

$$g = \frac{1-(a/b)^2}{2} - \frac{k}{k+1}\frac{\left[1-(a/b)^{k+1}\right]^2}{\left[1-(a/b)^{2k}\right]} + \frac{k(a/b)^2}{k-1}\frac{\left[1-(a/b)^{k-1}\right]^2}{\left[1-(a/b)^{2k}\right]} \tag{25}$$

Rewriting $\sigma'_r(r)$ (eq. (21)) in terms of b/a instead of a/b yields

$$\sigma'_r(r) = -\frac{M}{a^2hC}\left\{\left[\left(\frac{b}{a}\right)^{2k} - 1\right] - \left[\left(\frac{b}{a}\right)^{k+1} - 1\right]\left(\frac{r}{a}\right)^{k-1} - \left[\left(\frac{b}{a}\right)^{k-1} - 1\right]\left(\frac{b}{a}\right)^{k+1}\left(\frac{r}{a}\right)^{-(k+1)}\right\} \tag{26}$$

where

$$C \equiv \frac{1}{2}\left[\left(\frac{b}{a}\right)^2 - 1\right]\left[\left(\frac{b}{a}\right)^{2k} - 1\right] - \frac{k}{k+1}\left[\left(\frac{b}{a}\right)^{k+1} - 1\right]^2 + \frac{k}{k-1}\left(\frac{b}{a}\right)^2\left[\left(\frac{b}{a}\right)^{k-1} - 1\right]^2 \tag{27}$$

In dimensionless form, equation (26) may be written as

$$\frac{ha_m(b-a)}{M}\sigma'_r(r) = -\frac{(b/a)^2-1}{2C}\left\{\left[\left(\frac{b}{a}\right)^{2k} - 1\right] - \left[\left(\frac{b}{a}\right)^{k+1} - 1\right]\left(\frac{r}{a}\right)^{k-1} - \left[\left(\frac{b}{a}\right)^{k-1} - 1\right]\left(\frac{b}{a}\right)^{k+1}\left(\frac{r}{a}\right)^{-(k+1)}\right\} \tag{28}$$

where a_m is the radius of the middle surface of the curved bar given by

$$a_m = \frac{1}{2}(a+b) \tag{29}$$

For the isotropic case ($k = 1$), the equation may be expanded for $k \rightarrow 1$ in the following form for $h = 1$ (see app.):

$$[\sigma_r'(r)]_{k \rightarrow 1} = -\frac{4M}{Q}\left(\frac{a^2b^2}{r^2}\ln\frac{b}{a} + b^2\ln\frac{r}{b} + a^2\ln\frac{a}{r}\right) \tag{30}$$

where

$$Q = (b^2 - a^2)^2 - 4a^2b^2\left(\ln\frac{b}{a}\right)^2 \tag{31}$$

Equation (30) is exactly the same form as the stress equation given by Timoshenko and Goodier (1970) for isotropic materials.

Location of Maximum σ_r'

Differentiating equation (26) with respect to r, and setting the resulting derivative to zero,

$$\frac{d}{dr}[\sigma_r'(r)] = 0 \tag{32}$$

the radial location r_m' of the maximum σ_r' may be calculated as

$$\left(\frac{r_m'}{a}\right)^{2k} = \frac{(k+1)(b/a)^{k+1}\left[(b/a)^{k-1} - 1\right]}{(k-1)\left[(b/a)^{k+1} - 1\right]} \tag{33}$$

For the isotropic case $k \rightarrow 1$, equation (33) is reduced to

$$\left(\frac{r_m'}{a}\right)_{k \rightarrow 1} = \frac{b}{a}\sqrt{\frac{2\ln b/a}{(b/a)^2 - 1}} \tag{34}$$

where the relationship

$$\left\{\frac{\left[(b/a)^{k-1} - 1\right]}{k-1}\right\}_{k \rightarrow 1} = \frac{\ln(b/a)^{k-1}}{k-1} = \ln\frac{b}{a} \tag{35}$$

was used.

The peak radial stress $(\sigma_r')_{max}$ when $r = r_m'$ may be written as

$$\frac{ha_m(b-a)}{M}(\sigma_r')_{max} = -\frac{(b/a)^2 - 1}{2C}\left\{\left[\left(\frac{b}{a}\right)^{2k} - 1\right] - \left[\left(\frac{b}{a}\right)^{k+1} - 1\right]\left(\frac{r_m'}{a}\right)^{k-1} - \left[\left(\frac{b}{a}\right)^{k-1} - 1\right]\left(\frac{b}{a}\right)^{k+1}\left(\frac{r_m'}{a}\right)^{-(k+1)}\right\} \tag{36}$$

where r_m' is given in equation (33).

Thin Curved Bar

When the thickness of the bar is small (that is, $b \rightarrow a$), the expression C given in equation (27) may be expanded in terms of t/a (see eq. (16)) as

$$(C)_{b\rightarrow a} = -\frac{1}{6}k(k^2-1)\left(\frac{t}{a}\right)^4 + \cdots \tag{37}$$

in which all the lower order terms up to $O(t/a)^3$ cancelled out.

The expression for r'_{m} given in equation (33) could be expanded in a similar way to yield

$$\left(\frac{r'_{\mathrm{m}}}{a}\right)_{b\rightarrow a} = 1 + \frac{1}{2}\frac{t}{a} - \frac{5}{24}\left(\frac{t}{a}\right)^2 + \cdots \tag{38}$$

Equation (38) shows that the location of $(\sigma'_r)_{\max}$ is always on the inward side of the middle surface of the curved bar, and that the location of $(\sigma'_r)_{\max}$ drifts away from the middle surface more slowly than the case of $(\sigma_r)_{\max}$ (see eq. (18)) as the value b/a increases.

The stress equation (36) may be expanded in terms of t/a as

$$\left[\frac{ha_{\mathrm{m}}(b-a)}{M}(\sigma'_r)_{\max}\right]_{b\rightarrow a} = \frac{(1/2)k(k^2-1)(t/a)^4 + \cdots}{-2C} \tag{39}$$

Notice that all the terms up to $O(t/a)^3$ disappeared. With the application of equation (37), equation (39) becomes

$$\left[\frac{ha_{\mathrm{m}}(b-a)}{M}(\sigma'_r)_{\max}\right]_{b\rightarrow a} = \frac{3}{2} \tag{40}$$

which is independent of material anisotropy (that is, the value of k). Notice that the numerical values of both equations (20) and (40) are identical.

DELAMINATION STRESS

The open-mode maximum delamination stress σ_{D} induced in the curved bar under the end forces P with the loading axis offset e (see fig. 1) will be the sum of $(\sigma_r)_{\max}$ due to P without loading axis offset (eq. (15)) and $(\sigma'_r)_{\max}$ due to $M = Pe$ (eq. (36), see fig. 2):

$$\sigma_{\mathrm{D}} = (\sigma_r)_{\max} + (\sigma'_r)_{\max} \tag{41}$$

or

$$\sigma_{\mathrm{D}} = \frac{P}{h(b-a)}\left(F_1 + F_2\frac{e}{a_{\mathrm{m}}}\right) \tag{42}$$

where

$$F_1 = \frac{1}{B}\left(\frac{b}{a}-1\right)\frac{a}{r_m}\left[\left(\frac{r_m}{a}\right)^{\beta}+\left(\frac{b}{a}\right)^{\beta}\left(\frac{a}{r_m}\right)^{\beta}-\left(\frac{b}{a}\right)-1\right] \tag{43}$$

$$F_2 = -\frac{1}{2C}\left[\left(\frac{b}{a}\right)^2-1\right]\left\{\left[\left(\frac{b}{a}\right)^{2k}-1\right]-\left[\left(\frac{b}{a}\right)^{k+1}-1\right]\left(\frac{r'_m}{a}\right)^{k-1} - \left[\left(\frac{b}{a}\right)^{k-1}-1\right]\left(\frac{b}{a}\right)^{k+1}\left(\frac{r'_m}{a}\right)^{-(k+1)}\right\} \tag{44}$$

For thin-walled curved bar, the values of F_1 and F_2 are quite close, or

$$F_1 \approx F_2 \tag{45}$$

Therefore, the stress contribution from the end moments Pe for the thin-walled curved bar is almost proportional to the value of e/a_m.

NUMERICAL RESULTS

Figure 5 shows the dimensionless delamination stress $[h(b-a)/P](\sigma_r)_{max}$ induced by the end forces P plotted as a function of b/a for different values of anisotropic parameter β. As $b \rightarrow a$, the effect of anisotropy disappeared, and all the curves converge into a single point giving $\{[h(b-a)/P](\sigma_r)_{max}\}_{b\rightarrow a} = 1.5$, which has been established in equation (20). For low anisotropy $2 \leq \beta \leq 5$, the delamination stress increases monotonically with the increase of b/a. However, for high anisotropy of $\beta > 5$, the delamination stress curves show a slight valley (or dent) in the regions of moderate values of b/a. In these regions, $[h(b-c)/P](\sigma_r)_{max}$ yields values less than 1.5. Notice that as the value of β increases, the intensity of delamination stress decreases, and that the higher the value of b/a (that is, the thicker the wall), the higher the magnitude of the delamination stress.

Figure 6 shows the dimensionless radial distance $[(r_m/a)-1]/[(b/a)-1]$ of $(\sigma_r)_{max}$ point measured from the inner boundary of the curved bar plotted as a function of b/a. It is seen that the effect of anisotropy is relatively small and is negligible in the region $b/a < 1.4$. As the value of b/a increases, the location of $(\sigma_r)_{max}$ moves away from the middle surface and toward the inner boundary of the curved bar (see eq. (18)).

Figure 7 shows the plots of the dimensionless delamination stress $[ha_m(b-a)/M](\sigma'_r)_{max}$ induced by the end moments M as a function of b/a. Similar to the previous case, as $b/a \rightarrow 1$, all the stress curves converge into one point giving $[ha_m(b-a)/M](\sigma'_r)_{max} = 1.5$ which was established by equation (40). Notice that as the value of k increases, the magnitude of the delamination stress decreases. Figure 8 shows the dimensionless radial distance $[(r'_m/a)-1]/[(b/a)-1]$ of $(\sigma'_r)_{max}$ point measured from the inner boundary of the curved bar plotted as a function of b/a. The effect of anisotropy turned out to be very small and could be neglected in the region $1 < b/a < 1.7$. As b/a increases (that is, as the wall of the curved bar becomes thicker), the location of $(\sigma'_r)_{max}$ moved inwardly away from the middle surface with a slower rate as compared with figure 6 (compare eqs. (18) and (38)).

EXAMPLE

Let the curved bar be made of 25 composite plies with the stacking sequence of $[0_{10}/90/0/90/0/90/0_{10}]$, and with the following ply properties:

$$E_L = 25 \times 10^6 \text{ lb/in}^2 \tag{46}$$

$$E_T = 1.2 \times 10^6 \text{ lb/in}^2 \tag{47}$$

$$G_{LT} = 0.75 \times 10^6 \text{ lb/in}^2 \tag{48}$$

$$\nu_{LT} = 0.33 \tag{49}$$

$$\nu_{TL} = \nu_{LT}\frac{E_T}{E_L} = 0.01584 \tag{50}$$

where

E_L is modulus of elasticity of single ply in fiber direction,
E_T modulus of elasticity of single ply in the direction transverse to fiber direction,
G_{LT} shear modulus of single ply, and
ν_{LT},ν_{TL} Poisson's ratios of single ply.

Using the mixture rule, the elastic properties of the curved bar composite system may be calculated as

$$E_\theta = \frac{22}{25}E_L + \frac{3}{25}E_T = 22.144 \times 10^6 \text{ lb/in}^2 \tag{51}$$

$$E_r = E_T = 1.2 \times 10^6 \text{ lb/in}^2 \tag{52}$$

$$G_{\theta r} = G_{LT} = 0.75 \times 10^6 \text{ lb/in}^2 \tag{53}$$

$$\nu_{\theta r} = \frac{22}{25}\nu_{LT} + \frac{3}{25}\nu_{TL} = 0.2923 \tag{54}$$

where

E_θ is modulus of elasticity of laminated composite in θ direction,
E_r modulus of elasticity of laminated composite in r direction,
$G_{\theta r}$ shear modulus of laminated composite, and
$\nu_{\theta r}$ Poisson's ratio of laminated composite.

The two anisotropic parameters β and k of the composite system may be calculated as (see eqs. (5) and (24))

$$\beta = \sqrt{1 + \frac{E_\theta}{E_r}(1 - 2\nu_{\theta r}) + \frac{E_\theta}{G_{\theta r}}} = 6.1799 \tag{55}$$

$$k = \sqrt{\frac{E_\theta}{E_r}} = 4.2957 \tag{56}$$

It is seen that the composite system under consideration is highly anisotropic.

Let the mean radius a_m of the curved bar be chosen to be 1 in (ideal specimen size for common fatigue test machine, see fig. 1), then the inner and outer radii of the curved bar will be approximately (considering ply thickness ≈ 0.0118 in)

$$a = 0.085 \text{ in} \tag{57}$$

$$b = 1.15 \text{ in} \tag{58}$$

which give

$$b/a = 1.3529 \text{ in} \tag{59}$$

If the loading axis of P has an offset of

$$e = 0.375 \text{ in} \tag{60}$$

$(\sigma_r)_{max}$, $(\sigma'_r)_{max}$, r_m, and r'_m may be calculated respectively from equations (15), (36), (13), and (33) using the numerical values given above. The results are given in table 1, which includes the isotropic case for comparison.

TABLE 1—PEAK RADIAL STRESSES AND THEIR LOCATIONS

Items	Anisotropic ($\beta = 6.1799$, $k = 4.2957$)	Isotropic ($\beta = k = 1$)	Difference, percent
$[h(b-a)/P](\sigma_r)_{max}$	1.4939	1.5121	1.20
$[ha_m(b-a)/Pe](\sigma'_r)_{max}$	1.5093	1.5198	0.69
r_m (in)	0.9767	0.9774	0.07
r'_m (in)	0.9814	0.9812	0.02

Notice that the difference in the locations of $(\sigma_r)_{max}$ and $(\sigma'_r)_{max}$ is

$$r'_m - r_m = 0.9814 - 0.9767 = 0.0047 \text{ in} \tag{61}$$

which is about 40 percent of the ply thickness of 0.0118 in.

The maximum open-mode delamination stress σ_D induced by P and $M = Pe$ may be written as

$$\sigma_D = (\sigma_r)_{max} + (\sigma'_r)_{max} \tag{62}$$

or

$$\sigma_D = \frac{P}{h(b-a)}\left(1.4939 + 1.5093\frac{e}{a_m}\right) \tag{63}$$

$$= \frac{P}{h(b-a)}[1.4939 + 0.5660] \tag{64}$$

$$= \frac{P}{h(b-a)}[2.0599] \tag{65}$$

The contribution from the end moments $M = Pe$ is about 38 percent, and is roughly proportional to the value of e/a_m.

CONCLUDING REMARKS

Delamination stresses in a semicircular laminated composite curved bar subjected to end forces and end moments were calculated, and their radial locations were determined. A family of design curves was presented, showing the variation of the intensity of delamination stresses and their radial locations with different geometries and different degrees of anisotropy of the curved bar. The information provided can be used to select proper geometry of the curved bar fatigue test coupon and to optimize the composite stacking sequence so that delamination can initiate at the site of peak delamination stress.

APPENDIX—EXPANSION OF STRESS EQUATIONS (26) AND (27) FOR ISOTROPIC CASE ($k = 1$)

Equations (26) and (27) may be rewritten as (for $h = 1$)

$$\sigma_r'(r) = -\frac{M}{a^2 C}\left\{\left(\frac{b}{a}\right)^{2k} - 1 - \left[\left(\frac{b}{a}\right)^{k+1} - 1\right]\left(\frac{r}{a}\right)^{k-1} - \left[\left(\frac{b}{a}\right)^{k-1} - 1\right]\left(\frac{b}{a}\right)^{k+1}\left(\frac{r}{a}\right)^{-(k+1)}\right\} \tag{66}$$

$$C = \frac{1}{2}\left[\left(\frac{b}{a}\right)^2 - 1\right]\left[\left(\frac{b}{a}\right)^{2k} - 1\right] - \frac{k}{k+1}\left[\left(\frac{b}{a}\right)^{k+1} - 1\right]^2 + \frac{k}{k-1}\left(\frac{b}{a}\right)^2\left[\left(\frac{b}{a}\right)^{k-1} - 1\right]^2 \tag{67}$$

when $k \longrightarrow 1$, equations (66) and (67) may be expanded in the neighborhood of $k = 1$ as follows.

Expansion of C

For the small value of $(k - 1)$, equation (67) may be rewritten as

$$(C)_{k\longrightarrow 1} = \frac{1}{2}\left[\left(\frac{b}{a}\right)^2 - 1\right]\left[\left(\frac{b}{a}\right)^{2k} - 1\right] - \frac{1 + (k-1)}{2[1 + (k-1)/2]}\left[\left(\frac{b}{a}\right)^{k+1} - 1\right]^2 + \frac{k}{k-1}\left(\frac{b}{a}\right)^2\left[\ln\left(\frac{b}{a}\right)^{k-1}\right]^2 \tag{68}$$

where the relationship

$$\left[\left(\frac{b}{a}\right)^{k-1} - 1\right]_{k\longrightarrow 1} = \ln\left(\frac{b}{a}\right)^{k-1} \tag{69}$$

was used in the last term of equation (68).

Rearranging equation (69),

$$(C)_{k\longrightarrow 1} = \frac{1}{2}\left[\left(\frac{b}{a}\right)^2 - 1\right]\left[\left(\frac{b}{a}\right)^{2k} - 1\right] - \frac{1}{2}\left[\left(\frac{b}{a}\right)^{k+1} - 1\right]^2 - \frac{1}{4}(k-1)\left[\left(\frac{b}{a}\right)^{k+1} - 1\right]^2 + k(k-1)\left(\frac{b}{a}\right)^2\left[\ln\frac{b}{a}\right]^2 \tag{70}$$

or

$$(C)_{k\longrightarrow 1} = -(k-1)\left\{\frac{1}{4}\left[\left(\frac{b}{a}\right)^2 - 1\right]^2 - \left(\frac{b}{a}\right)^2\left[\ln\frac{b}{a}\right]^2\right\} \tag{71}$$

or

$$(C)_{k\longrightarrow 1} = -\frac{(k-1)}{4a^4}Q \tag{72}$$

where

$$Q = (b^2 - a^2)^2 - 4a^2b^2\left(\ln\frac{b}{a}\right)^2 \tag{73}$$

Expansion of σ'_r

With equation (72) considered, the stress equation (66) may be rewritten as

$$[\sigma'_r(r)]_{k\to 1} = \frac{4Ma^2}{(k-1)Q}\left\{\left[\left(\frac{b}{a}\right)^{2k}-1\right]\left[1-\frac{(b/a)^{k+1}-1}{(b/a)^{2k}-1}\left(\frac{r}{a}\right)^{k-1}\right]-\left[\left(\frac{b}{a}\right)^{k-1}-1\right]\left(\frac{b}{r}\right)^{k+1}\right\} \tag{74}$$

$$= \frac{4Ma^2}{(k-1)Q}\left\{\left[\left(\frac{b}{a}\right)^{2k}-1\right]\left[-\ln\frac{(b/a)^{k+1}-1}{(b/a)^{2k}-1}\left(\frac{r}{a}\right)^{k-1}\right]-\left(\frac{b}{r}\right)^{k+1}\ln\left(\frac{b}{a}\right)^{k-1}\right\} \tag{75}$$

$$= \frac{4Ma^2}{(k-1)Q}\left\{\left[\left(\frac{b}{a}\right)^{2k}-1\right]\left[-\ln\left(\frac{r}{a}\right)^{k-1}\right]-\left[\left(\frac{b}{a}\right)^{2k}-1\right]\ln\frac{(b/a)^{k+1}-1}{(b/a)^{2k}-1}\right.$$

$$\left.-\left(\frac{b}{r}\right)^{k+1}\ln\left(\frac{b}{a}\right)^{k-1}\right\} \tag{76}$$

$$= \frac{4Ma^2}{(k-1)Q}\left\{-(k-1)\left[\left(\frac{b}{a}\right)^{2k}-1\right]\ln\frac{r}{a}-(k-1)\left(\frac{b}{r}\right)^{k+1}\ln\frac{b}{a}\right.$$

$$\left.-\left[\left(\frac{b}{a}\right)^{2k}-1\right]\left[\frac{(b/a)^{k+1}-1}{(b/a)^{2k}-1}-1\right]\right\} \tag{77}$$

The last term of equation (77) may further be expanded as

$$-\left[\left(\frac{b}{a}\right)^{2k}-1\right]\left[\frac{(b/a)^{k+1}-1}{(b/a)^{2k}-1}-1\right] = \left(\frac{b}{a}\right)^{k+1}\left[\left(\frac{b}{a}\right)^{k-1}-1\right] = \left(\frac{b}{a}\right)^{k+1}\ln\left(\frac{b}{a}\right)^{k-1} \tag{78}$$

$$= \left(\frac{b}{a}\right)^{k+1}(k-1)\ln\frac{b}{a} \tag{79}$$

Thus equation (77) may be simplified to

$$[\sigma'_r(r)]_{k\to 1} = -\frac{4Ma^2}{Q}\left\{\left[\left(\frac{b}{a}\right)^{2k}-1\right]\ln\frac{r}{a}+\left(\frac{b}{r}\right)^{k+1}-\left(\frac{b}{a}\right)^{k+1}\ln\frac{b}{a}\right\} \tag{80}$$

or

$$[\sigma'_r(r)]_{k\to 1} = -\frac{4M}{Q}\left[\frac{a^2b^2}{r^2}\ln\frac{b}{a}+b^2\ln\frac{r}{b}+a^2\ln\frac{a}{r}\right] \tag{81}$$

which is the form of the stress equation given by Timoshenko and Goodier (1970) for isotropic curved bar under end moments M.

REFERENCES

Lekhnitskii, S.G.; Tsai, S.W.; and Cheron, T.: *Anisotropic Plates.* Gordon and Breach Science Publishers, New York, 1968.

O'Brien, T.K.: Characterization of delamination onset and growth in a composite laminate, in *Special Technical Testing Publication 775*, American Society for Testing and Materials, 1982, pp. 140–167.

O'Brien, T.K.: *Interlaminar Fracture of Composites.* NASA TM-85768, 1984a.

O'Brien, T.K.: Mixed-mode strain-energy-release rate effects on edge delamination of composites, in *Special Technical Testing Publication 836*, American Society for Testing and Materials, 1984b, pp. 125–142.

Timoshenko, S.P.; and Goodier, J.N.: *Theory of Elasticity.* McGraw-Hill Book Co., Inc., New York, 1970.

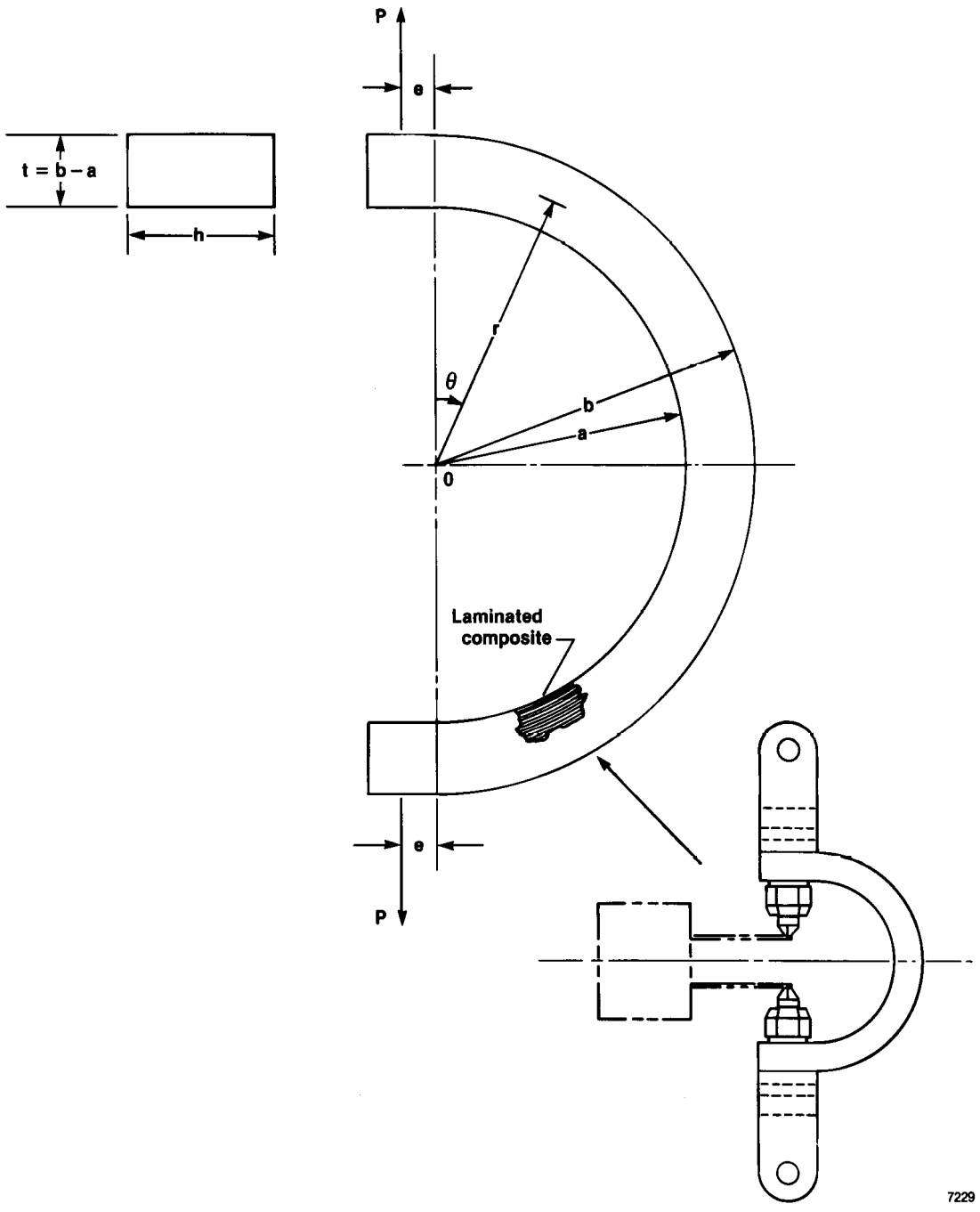

Figure 1. Laminated composite curved-bar test coupon for fatigue delamination study.

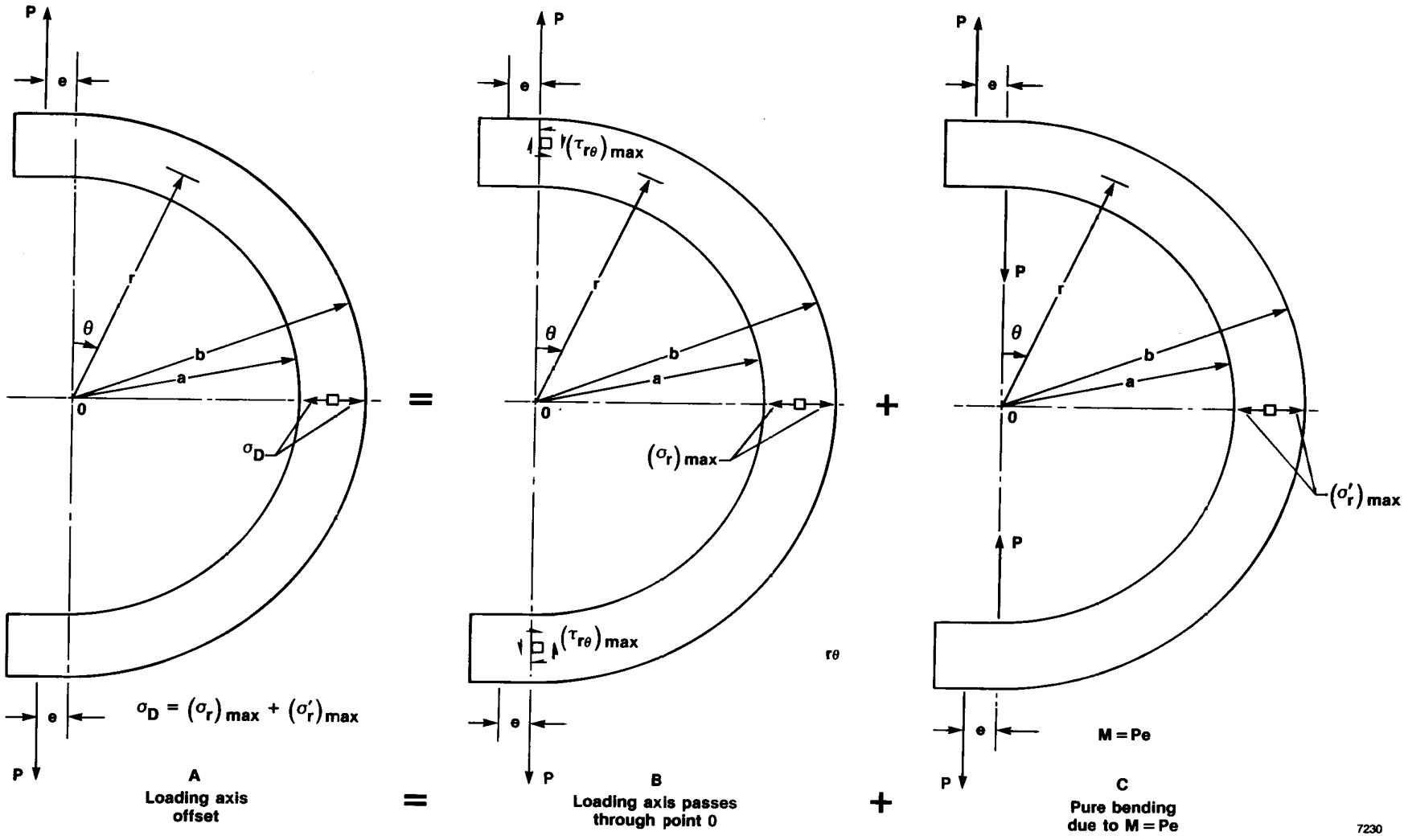

Figure 2. Bending of curved bar by forces at its ends. Loading axis has offset e.

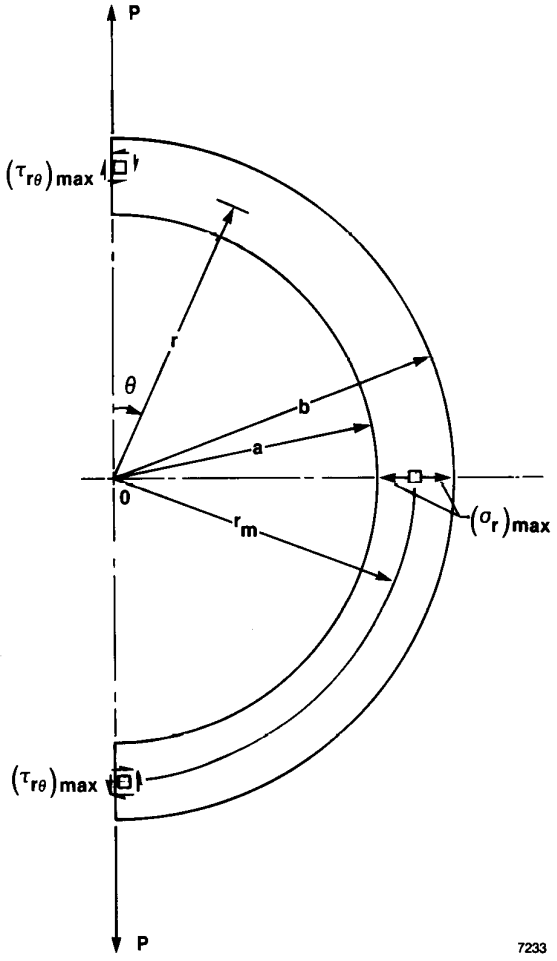

Figure 3. Bending of semicircular curved bar by forces at its ends (case of figure 2, B).

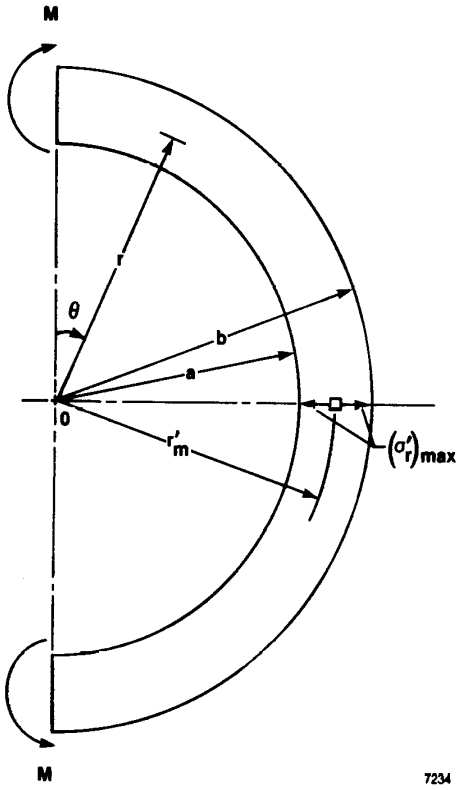

Figure 4. Bending of semicircular curved bar by moments at its ends (case of figure 2, C).

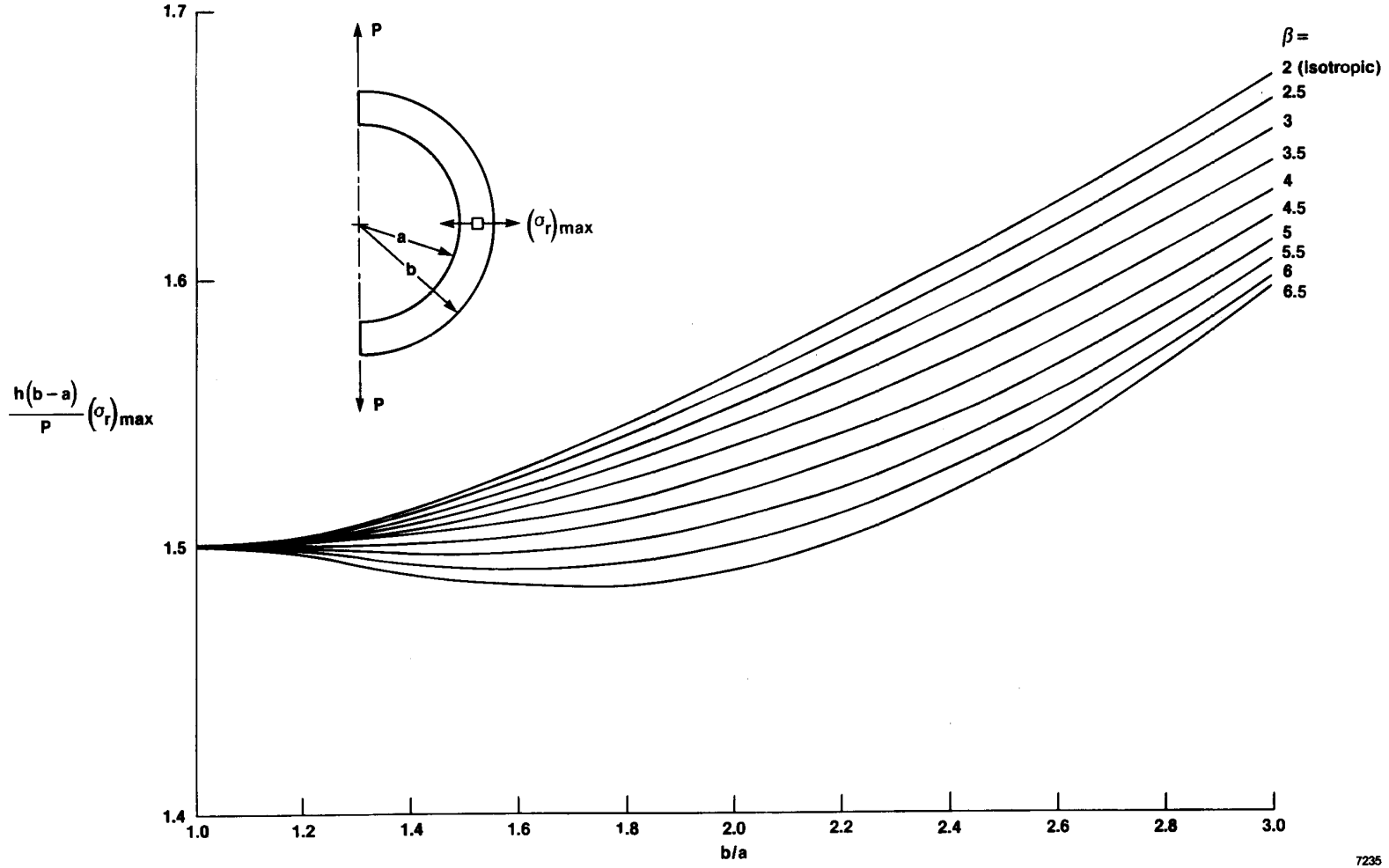

Figure 5. Plots of delamination stress $(\sigma_r)_{max}$ as a function of b/a for different values of β.

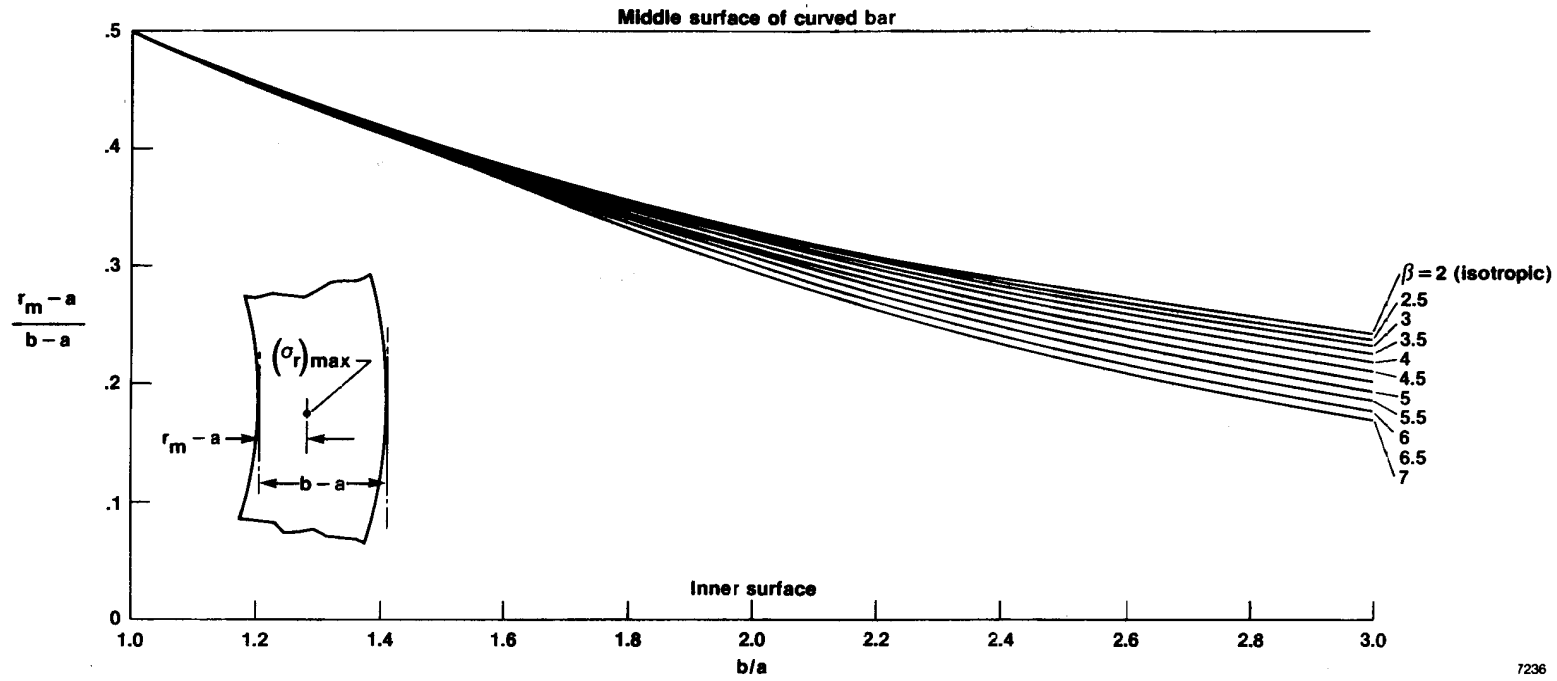

Figure 6. Plots of locations of $(\sigma_r)_{max}$ *as a function of* b/a *for different values of* β.

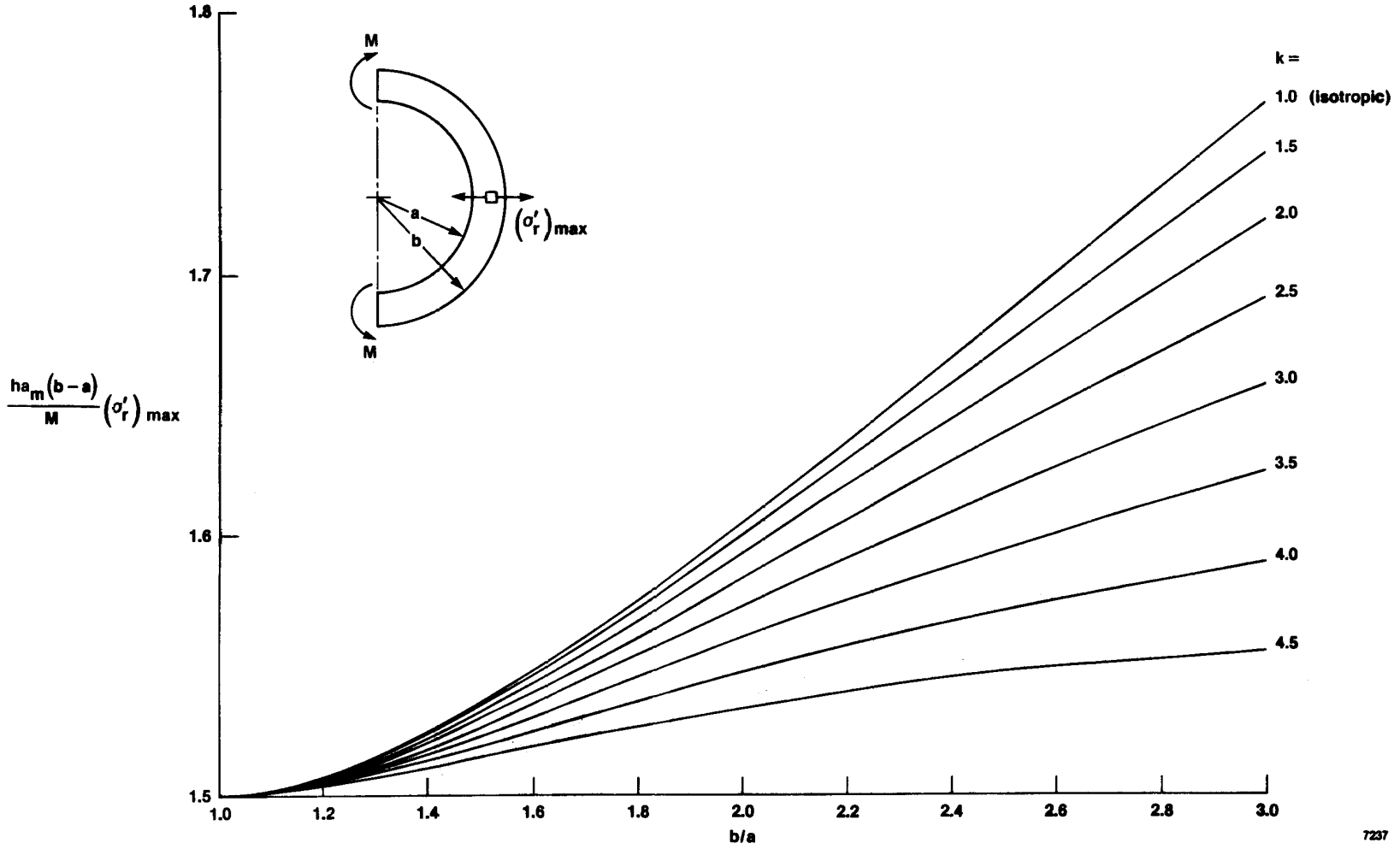

Figure 7. Plots of delamination stress $(\sigma'_r)_{max}$ *as a function of* b/a *for different values of* k.

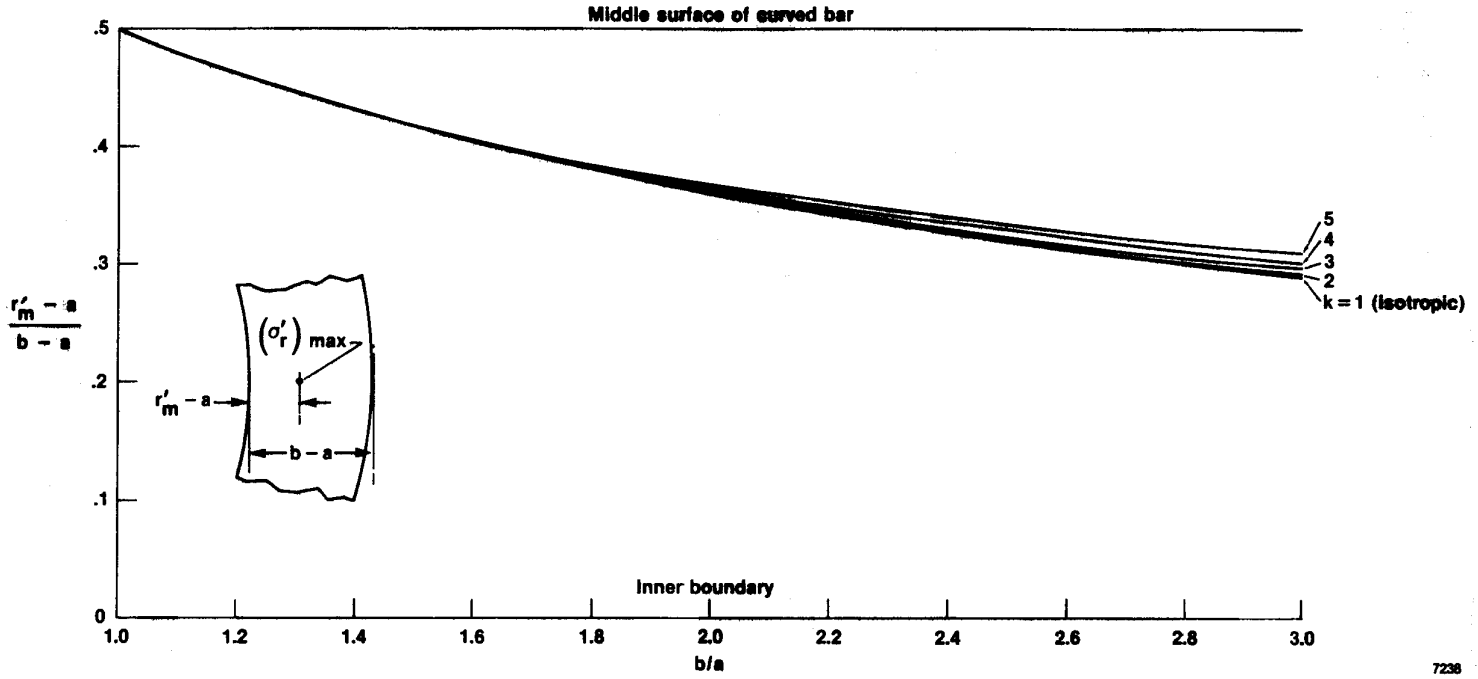

Figure 8. Plots of locations of $(\sigma'_r)_{max}$ as a function of b/a for different values of k.

1. Report No. NASA TM-4026	2. Government Accession No.	3. Recipient's Catalog No.
4. Title and Subtitle Delamination Stresses in Semicircular Laminated Composite Bars		5. Report Date January 1988 6. Performing Organization Code
7. Author(s) William L. Ko		8. Performing Organization Report No. H-1417
9. Performing Organization Name and Address NASA Ames Research Center Dryden Flight Research Facility P.O. Box 273, Edwards, CA 93523-5000		10. Work Unit No. RTOP 532-09-01 11. Contract or Grant No.
12. Sponsoring Agency Name and Address National Aeronautics and Space Administration Washington, DC 20546		13. Type of Report and Period Covered Technical Memorandum 14. Sponsoring Agency Code
15. Supplementary Notes		

16. Abstract

Using anisotropic elasticity theory, delamination stresses in a semicircular laminated composite curved bar subjected to end forces and end moments were calculated, and their radial locations were determined. A family of design curves was presented, showing variation of the intensity of delamination stresses and their radial locations with different geometry and different degrees of anisotropy of the curved bar. The effect of anisotropy on the location of peak delamination stress was found to be small.

17. Key Words (Suggested by Author(s))	18. Distribution Statement		
Delamination stresses Laminated composite Semicircular curved bar Stress analysis	Unclassified — Unlimited Subject Category 24		
19. Security Classif. (of this report) Unclassified	20. Security Classif. (of this page) Unclassified	21. No. of Pages 25	22. Price* A02

**For sale by the National Technical Information Service, Springfield, Virginia 22161.*

NASA-Langley, 1988